Nigerian Journal of Technology (NIJOTECH)
Vol. 40, No. 6 November, 2021, pp.1018 –1029
www.nijotech.com

Print ISSN: 0331-8443
Electronic ISSN: 2467-8821
http://dx.doi.org/10.4314/njt.v40i6.4

Elastic Bending Analysis Exact Solution of Plate using Alternative I Refined Plate Theory

F. C. Onyeka[1] and T. E Okeke[2, *]

[1,] *Department of Civil Engineering, Edo State University, Uzairue, Edo State, NIGERIA*
[2] *Department of Civil Engineering, University of Nigeria Nsukka, Enugu State, NIGERIA*

Abstract
Plate materials play a significant role in civil engineering and its application is found in building, bridges, marine, nuclear and structural engineering. Plates are three-dimensional (3-D) structural elements and normal practice in its analysis as two-dimensional (2-D) element has produced unreliable design which is a major problem in the construction industry. In this paper, a 3-D exact elastic plate theory (alternative I refined plate theory) is developed and applied to the bending analysis of an isotropic rectangular plate with free support at the third edge and the other edges clamped (CCFC) under uniformly distributed transverse load. The energy equation is formulated using the three-dimensional constitutive relations thereafter, the compatibility equation was obtained through general variation. The solution of the compatibility equation gave an exact deflection function of the plate as presented in the trigonometric form. This deflection function which is a product of the coefficient of deflection and shape function of the plate are substituted back into the energy equation, and simplified through minimization with respect to the coefficients of deflection and shear deformation to get a realistic formula for calculating the deflection, rotations and stresses of thick rectangular plate. The results of deflections and stresses obtained at aspect ratio of 2 were compared with those of previous studies available in the literature. It was observed that the present theory varied more with those of 2-D refined plate theory (RPT) with an assumed deflection function by 6.2% whereas it varied with exact 2-D RPT by 3.1%. This shows the inefficiency of assuming the deflection function in the analysis of thick plate. Meanwhile, the recorded total percentage differences showed that 2-D RPT over predicted the bending characteristics of the plate with 4.7%. This finding provides in-depth insight about the coarseness of 2-D RPT in the thick plate analysis.

Keywords: Exact solution of CCFC plate, alternative I refined plate theory (AIRPT), compatibility equation, elastic bending analysis and trigonometric displacement functions.

1.0 INTRODUCTION

The use of plate materials in engineering is on the increase over the years due to its attractive properties such as light weight, economy, its ability to withstand heavy loads and ability to tailor the structural properties [1 and 2]. They are used for the construction of civil engineering structures and other industrial applications, like bridges, roof, floor slabs, retaining walls, turbine disks, railways, ships dams, coaches, aircraft, etc., [3 and 4].

Plates are classified based on the nature of the deformation and material properties: orthotropic, isotropic, anisotropic plates, etc., and based on shape: rectangular, triangular, circular plates, etc. The support conditions at the edges of the plate can either be free, fixed or simply supported, etc. [5 and 6]. They can also be classified in terms of thickness (t) as; thin and thick plates, Anon [7]. Thin plate thickness is generally smaller than that of thick plate, the line perpendicular to the middle plane remains the same before and after deformation in thin plates. But in thick plates, the straight line at right angle to the middle surface before deformation does not remain the same after elongation. Thick plate has a wide range of applications due to its advantages such as: high mechanical properties, light weight, reduction in cost, heavy loads carrying capacities etc. [8].

The static flexural load carried by plates is usually perpendicular to the surface of the plate, Osadebe [5] and plates can have different supports at their edges, which can be fixed, simply supported, point, etc., just as seen in other structural elements like column, beams, etc. Due to the loads acting on a plate, stresses are developed [9], as such, it is important to carry out plate analysis in order to determine its ability to resist loads.

***Corresponding author **(Tel:** +234 (0) 8030405829**)**

Email addresses: *onyeka.festus@edouniversity.edu.ng* (Onyeka F.C), *edozie.okeke@unn.edu.ng* (Okeke, T. E)

Due to a wide application of thick plate in engineering and structures, various theories and approaches has been formulated and used in its analysis, for the determination of displacements, moments, stresses and stress resultants of the plates. Kirchhoff [10] formulated the classical plate theory (CPT) with the assumption that line which is normal to the neutral surface before deformation remain straight and normal on the neutral surface after deformation and it is mainly applied for the analysis of thin plate. The CPT has been found to be inadequate for the analysis of thick plates in that it doesn't put transverse shear deformation into consideration [11]. As a result, refined plate theory is developed which take care of transverse shear deformation effect on the plate structure.

First Order Shear Deformation Theory (FSDT) which is generally considered to be an improvement of CPT, and also considers transverse shear deformation in the analysis of plates. The FSDT has some limitation as it needs a shear correction factor. The limitation of the CPT and FSDTs led to the development of second order and higher order shear deformation theory [12 and 13]. These Higher Order Shear Deformation Theories (HSDT) give more accurate analysis results and also put transverse shear deformation into consideration by avoiding shear correction factors.

Mantari, *et al*. [14] and Sayyad, *et al.* [15] formulated a more accurate HSDT by using Exponential Shear Deformation Theory (ESDT) and Trigonometric Shear Deformation Theory (TSDT) in the analysis of isotropic plates subjected to uniformly distributed loads. Matikainen, *et al.* [16] used polynomial displacement functions in the analysis of thick plate.

Much work has not been carried out on the thick plate analysis considering the effect of shear deformation on the three directions (three-dimensional plate analysis). Few of them in the literature, the authors carried out the numerical analysis of plate like finite element method, finite strip method, etc. [6 and 17]. However, others try performing three-dimensional (3-D) analysis of solid rectangular plate by employing the Ritz approach which assumed the displacement function [18 and 19]. By assuming the displacement function, the result of the 3-D plate analysis will yield an approximate solution. Only Ibearugbulem, *et al.* [20] and Onyeka, *et al*. [21] utilized the analytical approach to get the exact displacement function from the governing equation (without assumption) in the bending analysis of thick rectangular plate. They did not apply trigonometric function which gives closer form solution than polynomial in the plate analysis [22]. Onyeka, *et al*. [21] used a 2-D model based on HSDT, they neglected the stresses along the thickness axis which made their solution not to be exact. Ibearugbulem, *et al.* [20] did not solve for plate with free support at the third edge and the other edges clamped (CCFC) boundary condition. This gap in the literature is worth filling.

In this study, an exact 3-D elastic plate theory (Alternative I RPT) will be analytically developed and applied it in the three-dimensional rectangular plate subjected to a uniform distributed load using trigonometric displacement functions. The aim of this work is to study an elastic bending analysis a thick rectangular plate by determining the exact displacement and stress solutions of the plate with a free support at the third edge and the other edges clamped boundary conditions using the general variation approach.

2.0 METHODOLOGY

Based on the general thick plate assumption, the energy equation of a thick rectangular plate is formulated following the kinematics and three-dimensional constitutive relations for a static elastic theory of plate.

2.1 Kinematics

In this section, the displacement field which includes the displacements along x, y and z-axes: u, v and w are obtained assuming that the x-z section and y-z section, which are initially normal to x-y plane before bending go off normal to x-y plane after bending of the plate (see Figure 1). As shown in figure 1, the spatial dimensions of the plate along x, y and z-axes are a, b and t respectively [22].

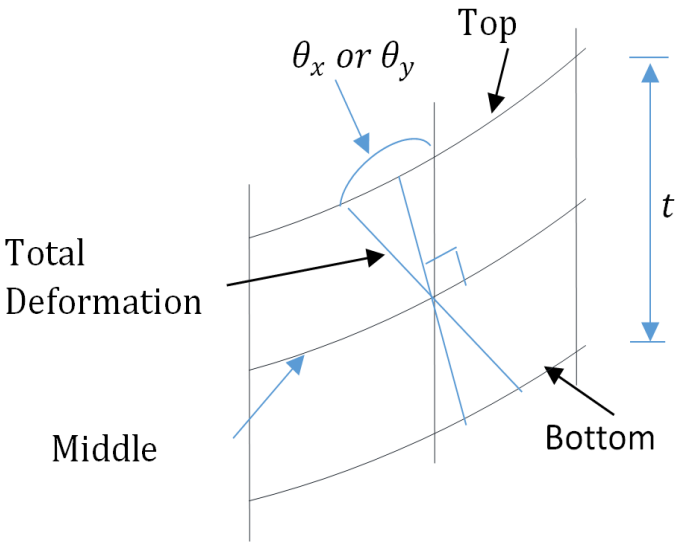

Figure 1: Rotation of x-z (or y-z) section after

From figure 1, the displacement and slope along the x axis and y axis are mathematically expressed as [22]:

$$\theta_x = \frac{\partial u}{\partial z} \quad (1)$$

$$\theta_y = \frac{\partial v}{\partial z} \quad (2)$$

Considering assumption iii and figure 1, F as used is a function of z coordinate. Thus, the in-plane displacements; u and v as presented in the Equation 2 and 3 are further defined using trigonometric relations for small angles as:

$$u = z\theta_x \quad (3)$$

$$v = z\theta_y \quad (4)$$

Where:
u and v is the in-plane displacement along x-axis and y axis respectively,
θ_x and θ_y is the shear deformation slope along x axis and y axis, and F represents the shear deformation profile.

Taking the non-dimensional form of coordinates to be R = x/a, Q = y/b and S = z/t corresponding to x, y and z-axes respectively, the six strain components in terms of non-dimensional coordinates are written as:

$$\varepsilon_x = \frac{St}{a}\frac{d\theta_x}{dR} \quad (5)$$

$$\varepsilon_y = \frac{St}{a\beta}\frac{d\theta_y}{dQ} \quad (6)$$

$$\varepsilon_z = \frac{1}{t}\frac{dw}{dS} \quad (7)$$

$$\gamma_{xy} = \frac{St}{a\beta}\frac{d\theta_x}{dQ} + \frac{St}{a}\frac{d\theta_y}{dR} \quad (8)$$

$$\gamma_{xz} = \theta_x + \frac{1}{a}\frac{dw}{dR} \quad (9)$$

$$\gamma_{yz} = \theta_y + \frac{1}{a\beta}\frac{dw}{dQ} \quad (10)$$

Where:

$\varepsilon_x, \varepsilon_y$ and ε_z are normal strain along x axis, y axis and z axis respectively,
γ_{xy}, γ_{xz} *and* γ_{yz} represents the shear strain in the plane parallel to the x-y, x-z and y-z plane.

2.2 Constitutive Relations

By considering the stresses causing the body movements, the generalized Hooke's law principle was applied to get the three dimensional constitutive relation as given in Equation 11:

$$\begin{bmatrix}\varepsilon_x\\ \varepsilon_y\\ \varepsilon_z\\ \gamma_{xz}\\ \gamma_{yz}\\ \gamma_{xy}\end{bmatrix} = \frac{1}{E}\begin{bmatrix}1 & -\mu & -\mu & 0 & 0 & 0\\ -\mu & 1 & -\mu & 0 & 0 & 0\\ -\mu & -\mu & 1 & 0 & 0 & 0\\ 0 & 0 & 0 & 2(1+\mu) & 0 & 0\\ 0 & 0 & 0 & 0 & 2(1+\mu) & 0\\ 0 & 0 & 0 & 0 & 0 & 2(1+\mu)\end{bmatrix}\begin{bmatrix}\sigma_x\\ \sigma_y\\ \sigma_z\\ \tau_{xz}\\ \tau_{yz}\\ \tau_{xy}\end{bmatrix} \quad (11)$$

Modulus of elasticity and Poisson's ratios are denoted with E and μ respectively.
Substituting Equations 5 to 10 into Equation 11 and writing the equations of the six stress components one by one in term of the displacements gives:

$$\sigma_x = \frac{Ets}{(1+\mu)(1-2\mu)a}\left[(1-\mu).\frac{\partial\theta_x}{\partial R} + \frac{\mu}{\beta}.\frac{\partial\theta_y}{\partial Q} + \frac{\mu a}{st^2}.\frac{\partial w}{\partial S}\right] \quad (12)$$

$$\sigma_y = \frac{Ets}{(1+\mu)(1-2\mu)a}\left[\mu.\frac{\partial\theta_x}{\partial R} + \frac{(1-\mu)}{\beta}.\frac{\partial\theta_y}{\partial Q} + \frac{\mu a}{st^2}.\frac{\partial w}{\partial S}\right] \quad (13)$$

$$\sigma_z = \frac{Ets}{(1+\mu)(1-2\mu)a}\left[\mu.\frac{\partial\theta_x}{\partial R} + \frac{\mu}{\beta}.\frac{\partial\theta_y}{\partial Q} + \frac{(1-\mu)a}{st^2}.\frac{\partial w}{\partial S}\right] \quad (14)$$

$$\tau_{xy} = \frac{E(1-2\mu)ts}{2(1+\mu)(1-2\mu)a}.\left[\frac{1}{\beta}\frac{\partial\theta_x}{\partial Q} + \frac{\partial\theta_y}{\partial R}\right] \quad (15)$$

$$\tau_{xz} = \frac{E(1-2\mu)ts}{2(1+\mu)(1-2\mu)a}.\left[\frac{a}{ts}\theta_x + \frac{1}{ts}\frac{\partial w}{\partial R}\right] \quad (16)$$

$$\tau_{yz} = \frac{E(1-2\mu)ts}{2(1+\mu)(1-2\mu)a}.\left[\frac{a}{ts}\theta_y + \frac{1}{\beta ts}\frac{\partial w}{\partial Q}\right] \quad (17)$$

2.3 Strain Energy

Strain energy is defined as the average of the product of stress and strain indefinitely summed up within the spatial domain of the body. This mathematically expressed as:

$$U = \frac{abt}{2}\int_0^1\int_0^1\int_{-0.5}^{0.5}\left(\sigma_x\varepsilon_x + \sigma_y\varepsilon_y + \sigma_z\varepsilon_z + \tau_{xy}\gamma_{xy} + \tau_{xz}\gamma_{xz} + \tau_{yz}\gamma_{yz}\right) dR\, dQ\, dS \quad (18)$$

Substituting Equations 5 to 10 and Equations 12 to 17 into Equation 18, simplifying and carrying out the integration of the outcome with respect to S considering that S = z/t gives:

$$\begin{aligned} U &= \frac{D^* ab}{2a^2}\int_0^1\int_0^1\left[(1-\mu)\left(\frac{\partial\theta_{sx}}{\partial R}\right)^2 + \frac{1}{\beta}\frac{\partial\theta_{sx}}{\partial R}.\frac{\partial\theta_{sy}}{\partial Q}\right. \\ &+ \frac{(1-\mu)}{\beta^2}\left(\frac{\partial\theta_{sy}}{\partial Q}\right)^2 + \frac{(1-2\mu)}{2\beta^2}\left(\frac{\partial\theta_{sx}}{\partial Q}\right)^2 \\ &+ \frac{(1-2\mu)}{2}\left(\frac{\partial\theta_{sy}}{\partial R}\right)^2 \\ &+ \frac{6(1-2\mu)}{t^2}\left(a^2{\theta_{sx}}^2 + a^2{\theta_{sy}}^2 + \left(\frac{\partial w}{\partial R}\right)^2 + \frac{1}{\beta^2}\left(\frac{\partial w}{\partial Q}\right)^2\right. \\ &+ 2a.\theta_{sx}\frac{\partial w}{\partial R} + \frac{2a.\theta_{sy}}{\beta}\frac{\partial w}{\partial Q}\Big) \\ &\left.+ \frac{(1-\mu)a^2}{t^4}\left(\frac{\partial w}{\partial S}\right)^2\right] dR\, dQ \end{aligned} \quad (19)$$

Where:

$$D^* = \frac{Et^3}{12(1+\mu)(1-2\mu)} = D\,\frac{(1-\mu)}{(1-2\mu)} \quad (20)$$

2.4 Energy Equation Formulation

Total Energy Expression be the algebraic summation of strain energy (U) and external work (E). That is:

$$\prod = \mathrm{U} - \mathrm{E} \quad (21)$$

The potential energy for the plate with uniformly distributed load is given as:

$$E = -\int_0^a\int_0^b qw(x,y)\partial x\partial y \quad (22)$$

Where; the symbol w(x,y) denotes the deflection in x and y direction, and
q denotes the uniformly distributed load

$$E = abq\int_0^1\int_0^1 w\, dR\, dQ \quad (23)$$

Where, the symbol h denotes the shape function of the plate, while; a and b is the length and breadth of the plate
Substituting Equations 19 and 22 into Equation 21 gives:

$$\begin{aligned} \Pi &= \frac{D^* ab}{2a^2}\int_0^1\int_0^1\left[(1-\mu)\left(\frac{\partial\theta_{sx}}{\partial R}\right)^2 + \frac{1}{\beta}\frac{\partial\theta_{sx}}{\partial R}.\frac{\partial\theta_{sy}}{\partial Q}\right. \\ &+ \frac{(1-\mu)}{\beta^2}\left(\frac{\partial\theta_{sy}}{\partial Q}\right)^2 + \frac{(1-2\mu)}{2\beta^2}\left(\frac{\partial\theta_{sx}}{\partial Q}\right)^2 \\ &+ \frac{(1-2\mu)}{2}\left(\frac{\partial\theta_{sy}}{\partial R}\right)^2 \\ &+ \frac{6(1-2\mu)}{t^2}\left(a^2{\theta_{sx}}^2 + a^2{\theta_{sy}}^2 + \left(\frac{\partial w}{\partial R}\right)^2 + \frac{1}{\beta^2}\left(\frac{\partial w}{\partial Q}\right)^2\right. \\ &+ 2a.\theta_{sx}\frac{\partial w}{\partial R} + \frac{2a.\theta_{sy}}{\beta}\frac{\partial w}{\partial Q}\Big) + \frac{(1-\mu)a^2}{t^4}\left(\frac{\partial w}{\partial S}\right)^2 \\ &\left.- \frac{2qa^4 w}{D^*}\right] dR\, dQ \end{aligned} \quad (25)$$

2.5 Governing Equation

The solution of the governing equation in trigonometric form is obtained according to Onyeka, *et al.* [23] by minimizing the total potential energy functional with respect to deflection to give the exact deflection equation, shear deformation rotation in x-axis and shear deformation rotation in y-axis as presented in Equation 26, 27 and 28 respectively:

$$w = [1\ R\ Cos(c_1R)\ Sin(c_1R)]\begin{bmatrix}a_0\\a_1\\a_2\\a_3\end{bmatrix} \times [1\ Q\ Cos(c_1Q)\ Sin(c_1Q)]\begin{bmatrix}b_0\\b_1\\b_2\\b_3\end{bmatrix} \quad (26)$$

$$\theta_x = \frac{c}{a}.\Delta_0.[1\ c_1Sin(c_1R)\ c_1Cos(c_1R)]\begin{bmatrix}a_1\\a_2\\a_3\end{bmatrix} \times [1\ Q\ Cos(c_1Q)\ \ Sin(c_1Q)]\begin{bmatrix}b_0\\b_1\\b_2\\b_3\end{bmatrix} \quad (27)$$

$$\theta_y = \frac{c}{a\beta}.\Delta_0.[1\ R\ Cos(c_1R)\ \ Sin(c_1R)]\begin{bmatrix}a_0\\a_1\\a_2\\a_3\end{bmatrix} \times [1 \quad c_1Sin(c_1Q)\ \ c_1Cos(c_1Q)]\begin{bmatrix}b_1\\b_2\\b_3\end{bmatrix} \quad (28)$$

Let:

$$w = A_1.h \quad (29)$$

$$\theta_x = \frac{A_2}{a}.\frac{\partial h}{\partial R} \quad (30)$$

$$\theta_y = \frac{A_3}{a\beta}.\frac{\partial h}{\partial Q} \quad (31)$$

Where; $A_1, A_2\ and\ A_3$ is the coefficient of deflection, coefficient of shear deformation along x axis and coefficient of shear deformation along y axis respectively.

Substituting Equation 29, 30 and 31 into 25, gives:

$$\begin{aligned}\Pi = \frac{D^*ab}{2a^4}\int_0^1\int_0^1\Bigg[&(1-\mu){A_2}^2\left(\frac{\partial^2h}{\partial R^2}\right)^2 \\ &+\frac{1}{\beta^2}\left[A_2.A_3+\frac{(1-2\mu){A_2}^2}{2}+\frac{(1-2\mu){A_3}^2}{2}\right]\left(\frac{\partial^2h}{\partial R\partial Q}\right)^2 \\ &+\frac{(1-\mu){A_3}^2}{\beta^4}\left(\frac{\partial^2h}{\partial Q^2}\right)^2 \\ &+6(1-2\mu)\left(\frac{a}{t}\right)^2\Bigg(\left[{A_2}^2+{A_1}^2+2A_1A_2\right].\left(\frac{\partial h}{\partial R}\right)^2 \\ &+\frac{1}{\beta^2}.\left[{A_3}^2+{A_1}^2+2A_1A_3\right].\left(\frac{\partial h}{\partial Q}\right)^2\Bigg) \\ &-\frac{2qa^4hA_1}{D^*}\Bigg]dR\,dQ\end{aligned} \quad (32)$$

Writing Equation 32 in more symbolized form gives:

$$\begin{aligned}\Pi = \frac{D^*ab}{2a^4}\Bigg[&(1-\mu){A_2}^2k_x \\ &+\frac{1}{\beta^2}\left[A_2.A_3+\frac{(1-2\mu){A_2}^2}{2}+\frac{(1-2\mu){A_3}^2}{2}\right]k_{xy}+\frac{(1-\mu){A_3}^2}{\beta^4}k_y \\ &+6(1-2\mu)\left(\frac{a}{t}\right)^2\Big(\left[{A_2}^2+{A_1}^2+2A_1A_2\right].k_z \\ &+\frac{1}{\beta^2}.\left[{A_3}^2+{A_1}^2+2A_1A_3\right].k_{2z}\Big) \\ &-\frac{2qa^4k_hA_1}{D^*}\Bigg]\end{aligned} \quad (33)$$

Where:

$$k_x = \int_0^1\int_0^1\left(\frac{\partial^2h}{\partial R^2}\right)^2 dRdQ \quad (34)$$

$$k_{xy} = \int_0^1\int_0^1\left(\frac{\partial^2h}{\partial R\partial Q}\right)^2 dRdQ \quad (35)$$

$$k_y = \int_0^1 \int_0^1 \left(\frac{\partial^2 h}{\partial Q^2}\right)^2 dRdQ \quad (36)$$

$$k_z = \int_0^1 \int_0^1 \left(\frac{\partial h}{\partial R}\right)^2 dRdQ \quad (37)$$

$$k_{2z} = \int_0^1 \int_0^1 \left(\frac{\partial h}{\partial Q}\right)^2 dRdQ;\ k_h = \int_0^1 \int_0^1 h\,.dRdQ \quad (38)$$

Minimizing Equation 33 with respect to A_2 gives:

$$\frac{\partial \Pi}{\partial A_2} = (1-\mu)A_2 k_x + \frac{1}{2\beta^2}[A_3 + A_2(1-2\mu)]k_{xy} + 6(1-2\mu)\left(\frac{a}{t}\right)^2 [A_2 + A_1].k_z = 0 \quad (34)$$

Minimizing Equation 33 with respect to A_3 gives:

$$\frac{\partial \Pi}{\partial A_2} = \frac{(1-\mu)A_3}{\beta^4} k_y + \frac{1}{2\beta^2}[A_2 + A_3(1-2\mu)]k_{xy} + \frac{6}{\beta^2}(1-2\mu)\left(\frac{a}{t}\right)^2 ([A_3 + A_1].k_{2z}) = 0 \quad (35)$$

Rewriting Equations 34 and 35 gives:

$$\left[(1-\mu)k_x + \frac{1}{2\beta^2}(1-2\mu)k_{xy} + 6(1-2\mu)\left(\frac{a}{t}\right)^2 k_z\right]A_2 + \left[\frac{1}{2\beta^2}k_{xy}\right]A_3 = \left[-6(1 - 2\mu)\left(\frac{a}{t}\right)^2 k_z\right]A_1 \quad (36)$$

$$\left[\frac{1}{2\beta^2}k_{xy}\right]A_2 + \left[\frac{(1-\mu)}{\beta^4}k_y + \frac{1}{2\beta^2}(1-2\mu)k_{xy} + \frac{6}{\beta^2}(1-2\mu)\left(\frac{a}{t}\right)^2 k_{2z}\right]A_3 = \left[-\frac{6}{\beta^2}(1 - 2\mu)\left(\frac{a}{t}\right)^2 k_Q\right]A_1 \quad (37)$$

Solving Equations 36 and 37 simultaneously gives:

$$A_2 = UA_1 \quad (38)$$

$$A_3 = VA_1 \quad (39)$$

Let:

$$U = \frac{(r_{12}r_{23} - r_{13}r_{22})}{(r_{12}r_{12} - r_{11}r_{22})} \quad (40)$$

$$V = \frac{(r_{12}r_{13} - r_{11}r_{23})}{(r_{12}r_{12} - r_{11}r_{22})} \quad (41)$$

Where:

$$r_{11} = (1-\mu)k_x + \frac{1}{2\beta^2}(1-2\mu)k_{xy} + 6(1-2\mu)\left(\frac{a}{t}\right)^2 k_z \quad (42)$$

$$r_{22} = \frac{(1-\mu)}{\beta^4}k_y + \frac{1}{2\beta^2}(1-2\mu)k_{xy} + \frac{6}{\beta^2}(1-2\mu)\left(\frac{a}{t}\right)^2 k_{2z} \quad (43)$$

$$r_{12} = r_{21} = \frac{1}{2\beta^2}k_{xy};\ r_{13} = -6(1-2\mu)\left(\frac{a}{t}\right)^2 k_z;\ r_{23} = r_{32} = -\frac{6}{\beta^2}(1-2\mu)\left(\frac{a}{t}\right)^2 k_{2z} \quad (44)$$

Minimizing Equation 33 with respect to A_1 gives:

$$\frac{\partial \Pi}{\partial A_1} = \frac{D^* ab}{2a^4}\left[6(1-2\mu)\left(\frac{a}{t}\right)^2\left([2A_1 + 2A_2].k_z + \frac{1}{\beta^2}.[2A_1 + 2A_3].k_{2z}\right) - \frac{2qa^4 k_h}{D^*}\right] = 0 \quad (45)$$

That is:

$$6(1-2\mu)\left(\frac{a}{t}\right)^2\left([A_1 + UA_1].k_z + \frac{1}{\beta^2}.[A_1 + VA_1].k_{2z}\right) - \frac{qa^4 k_h}{D^*} = 0 \quad (46)$$

Factorizing Equations 46 and simplifying gives:

$$6(1-2\mu)\left(\frac{a}{t}\right)^2 A_1\left([1 + U].k_z + \frac{1}{\beta^2}.[1 + V].k_{2z}\right) = \frac{qa^4 k_h}{D^*} \quad (47)$$

$$TA_1 = \frac{qa^4 k_h}{D^*} \quad (48)$$

$$A_1 = \frac{qa^4}{D^*}\left(\frac{k_h}{T}\right) \quad (49)$$

Where:

$$T = 6(1-2\mu)\left(\frac{a}{t}\right)^2 * \left([1+G_2].k_z + \frac{1}{\beta^2}.[1+G_3].k_{2z}\right) \quad (50)$$

2.6 Exact Displacement and Stress Expression

By substituting the value of A_1, A_2 *and* A_3 in Equation 49, 38 and 39 into Equation 13 – 17, simplify appropriately, we have:

$$u = \mathrm{z}\,\frac{A_2}{\mathrm{a}}\,\frac{dh}{dR} \quad (51)$$

$$w = (R - 2R^3 + R^4) \times (Q - 2Q^3 + Q^4)A_1 \quad (52)$$

$$\sigma_x = \frac{\mathrm{Ets}}{(1+\mu)(1-2\mu)\mathrm{a}}\left[A_2\frac{\partial^2 h}{\partial R^2} + \mu\,\frac{A_3}{\beta^2}\,\frac{d^2 h}{dQ^2} + \frac{(1-\mu)\mathrm{a}}{s\mathrm{t}^2}.\frac{\partial \mathrm{w}}{\partial \mathrm{S}}\right] \quad (53)$$

$$\sigma_z = \frac{\mathrm{Ets}}{(1+\mu)(1-2\mu)\mathrm{a}}\left[\mu.\frac{\partial^2 h}{\partial R^2} + \frac{\mu}{\beta}.\frac{\partial^2 h}{\partial Q^2} + \frac{(1-\mu)\mathrm{a}}{s\mathrm{t}^2}.\frac{\partial \mathrm{w}}{\partial \mathrm{S}}\right] \quad (54)$$

$$\tau_{xy} = \frac{\mathrm{Ets}}{2(1+\mu)(1-2\mu)}.\frac{1}{\beta a^3}[A_2 + A_3]\frac{\partial^2 h}{\partial R\,\partial Q} \quad (55)$$

$$\tau_{yz} = \frac{\mathrm{Ets}}{2(1+\mu)(1-2\mu)}.\frac{1}{\beta a^2}.\left[A_1 + \frac{A_3}{t}\frac{\partial F}{dS}\right]\frac{\partial h}{\partial Q} \quad (56)$$

3.0 NUMERICAL ANALYSIS

The analysis of a thick rectangular SSSS plate whose Poisson's ratio is 0.3 and carrying uniformly distributed load (including self-weight) is presented. This is done by determining the deflection, w where R = 0.5, Q = 0.5 and S = 0; normal in-plane stresses σx, and σy, where R = 0.5, Q = 0.5 and S = 0.5; x-y plane shear stress τxy where R = 0, Q = 0 and S = 0.5; x-z plane shear stress τxz

where R= 0, Q = 0.5 and S = 0. The trigonometric shape function as was obtained in the previous section is subjected to the rectangular SSSS plate boundary condition shown on Figure 2 for various aspect ratios and span-depth ratio.

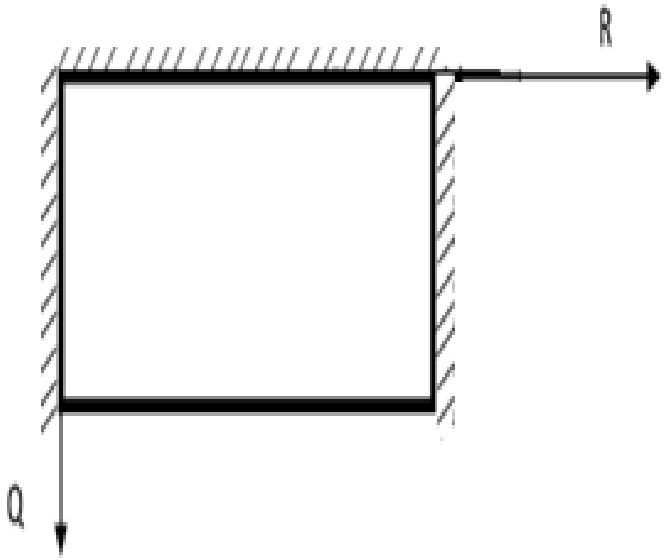

Figure 2: CCFC Rectangular Plate

The trigonometric exact displacement function for the plate analysis as derived in Equation 26 is given as presented in Equation (57).

$$w = (a_0 + a_1 R + a_2 \cos g_1 R + a_3 \sin g_1 R) \times (b_0 + b_1 Q + b_2 \cos g_2 Q + b_3 \sin g_2 Q) \quad (57)$$

The boundary conditions of the plate in figure 3 are as follows:

$$\text{At } R = Q = 0;\ w = 0 \quad (58)$$

$$\text{At } R = Q = 0;\ \frac{dw}{dR} = \frac{dw}{dQ} = 0 \quad (59)$$

$$\text{At } R = Q = 1;\ w = 0 \quad (60)$$

$$\text{At } R = Q = 1;\ \frac{dw}{dR} = \frac{dw}{dQ} = 0 \quad (61)$$

The trigonometric displacement $w\ (x, y)$ functions that satisfy the boundary conditions for one edge free and other three edges clamped rectangular plate boundary conditions are determined as follows:

Substituting Equation 58 to 61 into the derivatives of w and solving gave the characteristic equation as:

$$2Cos\ g_1 + g_1\ Sin\ g_1 - 2 = 0;\ b_2 Cos\ g_1 = 0 \quad (62)$$

The value of g_1 that satisfies Equation (62) is:

$$g_1 = 2m\pi;\ g_1 = \frac{n\pi}{2}[where\ m = n = 1, 2, 3 \ldots] \quad (63)$$

Substituting Equation (63) into the derivatives of w and satisfying the boundary conditions of Equation (58) to (61) gives the following constants;

$$a_1 = a_3 = b_3 = 0;\ b_1 = -g_1\ b_3 = 0;\ a_0 = -a_2; b_0 = -b_2 \quad (64)$$

Substituting the constants of Equation (63) and (64) into Equation (57) gave;

$$w = a_0(1 - Cos2m\pi R) \times b_0\left(1 - Cos\frac{n\pi Q}{2}\right) \quad (65)$$

Similarly;

$$w = a_2(Cos2m\pi R - 1) \times b_2\left(Cos\frac{n\pi Q}{2} - 1\right) \quad (66)$$

Recall from Equation (45), that;

$$w = A_1 h$$

Let $m = 1$

Therefore:

$$w = a_2 \times b_2(Cos2\pi R - 1).\left(Cos\frac{n\pi Q}{2} - 1\right) \quad (67)$$

Let the amplitude,

$$A_1 = a_2 \times b_2 \quad (68)$$

$$h = (Cos2\pi R - 1).\left(Cos\frac{n\pi Q}{2} - 1\right) \quad (69)$$

Thus, the trigonometric deflection functions after satisfying the boundary conditions is:

$$w = A_1(Cos2\pi R - 1).\left(Cos\frac{n\pi Q}{2} - 1\right) \quad (70)$$

Thus; using Equation (34),(35), (36), (37) and (38), the stiffness coefficients of CCFC rectangular plate is obtained and presented in the Table 1.

Table 1: Trigonometric form of stiffness coefficients of CCFC rectangular plate

Deflection form	k_x	k_{xy}	k_y	k_z	k_{2z}
Trigonometry	$80\pi^4$	$\frac{\pi^4}{4}$	$\frac{3\pi^4}{64}$	$\frac{9\pi^2}{20}$	$\frac{3\pi^2}{16}$

4.0 RESULTS AND DISCUSSIONS

The values of trigonometric stiffness coefficient displacement shape functions are presented in Table 1. The numerical results of displacements and stresses for the three dimensional isotropic plate subjected to a uniform distributed load are presented in non-dimensional form in Tables 2 and 3. To determine the correctness of the results from the present studies, comparison was made between values from the present study and those of past scholars.

The comparative analysis of non-dimensional in-plane displacement at the given coordinate positions for the span-to-thickness ratios $\left(\beta = \frac{a}{t}\right)$ from 4 to 9, 10, 20, 30, 40, 50, 60, 70, 80, 90, 100 and 1000 are presented in Tables 4. The in-plane displacement have compared those of CPT, 2-D HSDT by Gwarah [24], and an elasticity solution for pure bending analysis of plate Onyeka, *et al.* [21] and presented in terms of percentage error calculations.

From a critical look at table 2 and 3, it is shown that the value of in-plane displacement characteristics along x and y axis (u, v) increases as the span-thickness ratio increases while that the value of out of plane displacement characteristics (w) decreases as the span-thickness ratio increases. It is also observed in the table that the in-plane displacement along x and y axis (u, v) values decreases as the length to breadth ratio increases while out of plane displacement (w) value increases as the length to breadth ratio increases. This could imply that, the axial displacement is functions of x, y and z as it varies with the plate thickness while the deflection is only a function of x and y and did not vary linearly with the thickness of the plate thickness.

Furthermore, it was deduced from the Table 2 and 3 that the normal stress along x and y axis (σ_x *and* σ_y) and shear stress in the plane parallel to the x-y plane (τ_{xy}) increases as the span-thickness ratio increases while the shear stress in the plane parallel to the x-z and y-z plane (τ_{xz} *and* τ_{yz}) decreases as the span-thickness ratio increases. It is also observed that the values of these stresses $(\sigma_x, \sigma_y, \tau_{xy}, \tau_{xz}$ *and* $\tau_{yz})$ increase as the length to breadth ratio ($\propto = b/a$) of the plate increases. This implies that, as the length of the plate material increases, more stresses are induced in the plate which consequently leads to the failure of the plate material.

Looking at the tables 4, it is observed that as the span-to-thickness ratio increases, the values of in-plane displacement in the present study, which used exact 3-D elasticity theories gets close to those obtained from the past scholars that used classical plate theory and the 2-D refined thick plate theories (Gwarah [24] Onyeka, *et al.* [21]). The thickest plate (a/t of 4) has a percentage

difference of 5.1% (Onyeka, *et al.* [21]) and 21.4% (Gwarah [24]) with the present study. The lightest plate (a/t of 1000) has a percentage difference of 0 (Onyeka, *et al.* [21]) and 0.03% (Gwarah, [24]), which gives the same difference when compared with the value of the CPT. It is also, showed that at a span - thickness ratio above 100, the values obtained from the models used herein almost coincide with the values from the RPT and CPT. This is quite expected since we assumed in CPT analyses that at span-thickness ratios of 100 and above, a plate can be taken as being thin.

The comparative analysis performed as presented in the table 3 showed that the overall average percentage difference values of displacement obtained by present theory and those of Onyeka, *et al.* [21] and Gwarah [24] are 3.1% and 6.2% respectively. This means that the analytical 2-D RPT with exact displacement function (Onyeka, *et al.* [21]) gives a closer result when compared with exact 3-D plate theory (Alternative I, RPT) than that of Gwarah [24] which used an assumed displacement function in the analysis. Meanwhile, the values predicted by the present theory are in close agreement with previous scholars. The slightly higher average percentage difference of 6.2% showed the coarseness of refined plate theories in the thick plate analysis as they underestimate the stresses in the plate structure. Hence, the need to employ a typical 3-D with exact displacement function for plate analysis to achieve efficiency.

The present study converges with previous work as the span to thickness ratio increases and becomes the same or equal to CPT value at span to thickness ratio of 100. The rate of convergence can be seen in Figure 3. The total average percentage difference between the present study and that of previous studies is 4.7%. This means that at about 95% confidence level, the values from the present study are the same with those of previous studies. This higher confidence level proved that the present model (AIRPT) can be used with confidence for stress and bending analysis of thick rectangular plate that is clamped at the three edges and free of support at the other edge.

Table 2: Displacement and Stresses of CCFC plate for length to breadth ratio ($\propto = b/a$) of 2.0

	$\propto = 2.0$							
$\beta = \frac{a}{t}$	w	u	v	σ_x	σ_y	τ_{xy}	τ_{xz}	τ_{yz}
4	0.016715	-0.003999	-0.008990	0.256405	0.141043	-0.063781	0.016624	0.023142
5	0.013512	-0.003456	-0.007401	0.218636	0.118105	-0.053364	0.007347	0.009496
6	0.012075	-0.003456	-0.007401	0.218636	0.118105	-0.053364	0.007347	0.009496
7	0.011222	-0.003346	-0.007062	0.210928	0.113312	-0.051184	0.005437	0.006884
8	0.010675	-0.003275	-0.006840	0.205980	0.110209	-0.049772	0.004207	0.005247
9	0.010302	-0.003227	-0.006688	0.202613	0.108086	-0.048806	0.003368	0.004152
10	0.010036	-0.003193	-0.006579	0.200217	0.106568	-0.048115	0.002770	0.003383
20	0.009193	-0.003085	-0.006227	0.192622	0.101720	-0.045906	0.000868	0.001003
30	0.009038	-0.003065	-0.006162	0.191227	0.100823	-0.045497	0.000518	0.000576
40	0.008984	-0.003059	-0.006139	0.190740	0.100509	-0.045354	0.000395	0.000428
50	0.008959	-0.003055	-0.006128	0.190514	0.100363	-0.045288	0.000339	0.000359
60	0.008946	-0.003054	-0.006122	0.190392	0.100284	-0.045252	0.0003079	0.0003223
70	0.008937	-0.003053	-0.006119	0.190318	0.100237	-0.04523	0.0002894	0.0002999
80	0.008932	-0.003052	-0.006116	0.190270	0.100206	-0.045216	0.0002773	0.0002854
90	0.008928	-0.003051	-0.006115	0.190237	0.100185	-0.045207	0.0002691	0.0002754
100	0.008926	-0.003051	-0.006114	0.190214	0.100169	-0.045200	0.0002632	0.0002683
1000	0.008926	-0.003051	-0.006114	0.190214	0.100169	-0.045200	0.0002632	0.0002683
CPT	0.008926	-0.003051	-0.006114	0.190214	0.100169	-0.045200	0.0002632	0.0002683

Table 3: Displacement and Stresses of CCFC plate for length to breadth ratio ($\propto = b/a$) of 2.0

$\propto = 2.0$								
$\beta = \frac{a}{t}$	w	u	v	σ_x	σ_y	τ_{xy}	τ_{xz}	τ_{yz}
4	0.019368	-0.004413	-0.005713	0.282623	0.104958	-0.038818	0.018687	0.008563
5	0.016204	-0.003986	-0.004967	0.25509	0.093972	-0.03426	0.011808	0.005176
6	0.014539	-0.003762	-0.004565	0.240605	0.088156	-0.031825	0.008186	0.003518
7	0.013553	-0.00363	-0.004323	0.232024	0.084698	-0.03037	0.006040	0.002581
8	0.012920	-0.003545	-0.004166	0.226516	0.082473	-0.029429	0.004662	0.001998
9	0.012489	-0.003487	-0.004058	0.222766	0.080955	-0.028787	0.003723	0.001611
10	0.012182	-0.003446	-0.003981	0.220098	0.079874	-0.028328	0.003056	0.001339
20	0.011210	-0.003349	-0.003736	0.211639	0.076439	-0.026867	0.000938	0.000505
30	0.011031	-0.003315	-0.00369	0.210084	0.075806	-0.026597	0.000549	0.000356
40	0.010969	-0.003291	-0.003674	0.209541	0.075585	-0.026502	0.000413	0.0003042
50	0.01094	-0.003283	-0.003667	0.20929	0.075483	-0.026459	0.000350	0.0002803
60	0.010924	-0.003279	-0.003663	0.209154	0.075427	-0.026435	0.0003156	0.0002674
70	0.010915	-0.003277	-0.003661	0.209072	0.075394	-0.026421	0.000295	0.0002596
80	0.010909	-0.003275	-0.003659	0.209018	0.075372	-0.026411	0.0002817	0.0002545
90	0.010904	-0.003275	-0.003658	0.208982	0.075357	-0.026405	0.0002725	0.000251
100	0.010901	-0.003274	-0.003657	0.208955	0.075347	-0.0264	0.0002659	0.0002486
1000	0.010901	-0.003274	-0.003657	0.208955	0.075347	-0.0264	0.0002659	0.0002486
CPT	0.010901	-0.003272	-0.003657	0.208955	0.075347	-0.0264	0.0002659	0.0002486

Table 4: Comparative analysis of present study for length to breadth ratio ($\propto = b/a$) of 2.0 and past studies showing their percentage difference calculations at varying span-depth ratio ($\beta = a/t$).

$\propto = 2.0$						
$\beta = \frac{a}{t}$	**Present work** (u)	**Onyeka, *et al.* [21]** (u)	**Percentage difference** (%)	**Present work** (u)	**Gwarah [24]** (u)	**Percentage difference** (%)
4	-0.004651	-0.004413	-5.11718	-0.004413	-0.003654	-21.4363
5	-0.00421	-0.003986	-5.32067	-0.003986	-0.003517	-16.4608
6	-0.003971	-0.003762	-5.26316	-0.003762	-0.003442	-13.3216
7	-0.003835	-0.00363	-5.3455	-0.00363	-0.003397	-11.4211
8	-0.003751	-0.003545	-5.49187	-0.003545	-0.003368	-10.2106
9	-0.003692	-0.003487	-5.55255	-0.003487	-0.003348	-9.31744
10	-0.003631	-0.003446	-5.09502	-0.003446	-0.003333	-8.20711
20	-0.003571	-0.003349	-6.21675	-0.003349	-0.003299	-7.61691
30	-0.003518	-0.003315	-5.77032	-0.003315	-0.003287	-6.56623
40	-0.003412	-0.003291	-3.54631	-0.003291	-0.003279	-3.89801
50	-0.003385	-0.003283	-3.01329	-0.003283	-0.003274	-3.27917
60	-0.00328	-0.003279	-0.03049	-0.003279	-0.003274	-0.18293
70	-0.003278	-0.003277	-0.03051	-0.003277	-0.003274	-0.12203
80	-0.003277	-0.003275	-0.06103	-0.003275	-0.003273	-0.12206
90	-0.003276	-0.003275	-0.03053	-0.003275	-0.003273	-0.09158
100	-0.003275	-0.003274	-0.03053	-0.003274	-0.003273	-0.06107
1000	-0.003274	-0.003274	0	-0.003274	-0.003273	-0.03054
CPT	-0.003272	-0.003272	0	-0.003272	-0.003272	0
Average % difference		3.1			6.2	
Average total % difference			4.7			

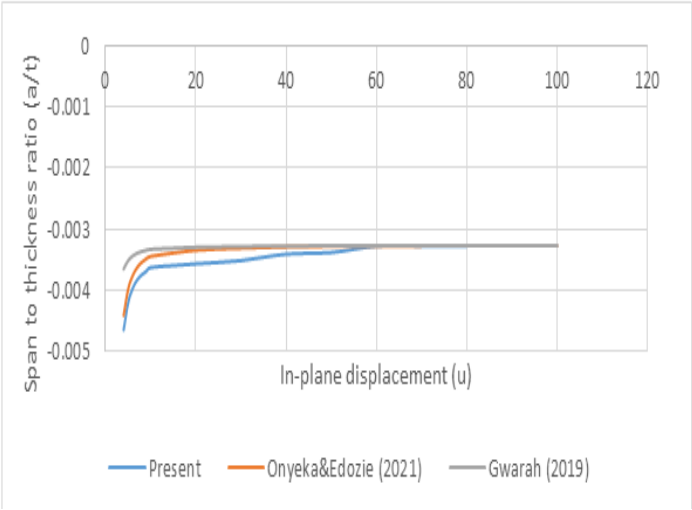

Figure 3: Graph of out-of-plane displacement (w) versus span to thickness ratio (a/t)

5.0 CONCLUSION AND RECOMMENDATION

The 3-D exact theory is a plate theory that involves all the six strains $(\varepsilon_x, \varepsilon_y, \varepsilon_z, \gamma_{xy}, \gamma_{xz}\ and\ \gamma_{yz})$ and stress $(\sigma_x, \sigma_y, \sigma_z, \tau_{xy}, \tau_{xz}\ and\ \tau_{yz})$ components in the analysis. Hence, they include more modulus of elasticity (E) and other mechanical properties of the plate. As a consequence, the proposed 3-D approach always predicts buckling load greater than those predicted by CPT and RPT because of these additional load (stresses), modulus of elasticity (E) and other mechanical properties of the plate.

From the result of percentage difference recorded, it can be concluded that the CPT and 2D RPT is only an approximate relation for buckling analysis of thick plate (although it turns out to be exact in the case of pure bending). Furthermore, the trigonometric displacement shear deformation theory developed to give a close form solution, thereby considered more accurate and safer for complete exact three-dimensional thick plate analysis. Its use in the analysis of thick plates will yield almost an exact result. Thus, confirming that the exact 3-D plate theory using trigonometric displacement function provides a good solution for the stability analysis of plates and, can be recommended for analysis of any type of rectangular plate under the same loading and boundary condition.

REFERENCES

[1] Gajbhiye, Param D., Vishisht Bhaiya, and Yuwaraj M. Ghugal "Free Vibration Analysis of Thick Isotropic Plate by Using 5th Order Shear Deformation Theory," *Progress in Civil and Structural Engineering*, 2021, pp 1–11. DOI:10.38208/pcse.v1i1.2

[2] Onyeka, F. C. and Edozie, O. T. "Application of higher order shear deformation theory in the analysis of thick rectangular plate," *International Journal on Emerging Technologies*, 11(5), 2020, pp 62–67.

[3] Shimpi, R. P., H. G. Patel, and H. Arya. "New First-Order Shear Deformation Plate Theories," *Journal of Applied Mechanics*, 74(3), 2006, pp 523–533. DOI:10.1115/1.2423036.

[4] Onyeka, F. C. Okafor, F. O. and Onah, H. N. "Displacement and Stress Analysis in Shear Deformable Thick Plate," *International Journal of Applied Engineering Research*, 13(11), 2018, pp 9893-9908.

[5] Osadebe N. N. Ike C. C. Onah H. N. Nwoji C. U. and Okafor F. O. "Application of the Galerkin-Vlasov Method to the Flexural Analysis of Simply Supported Rectangular Kirchhoff Plates under Uniform Loads," *Nigerian Journal of Technology*, 35(4), 2016, pp 732. DOI:10.4314/njt.v35i4.7

[6] Shwetha, K., Subrahmanya, V. and Bhat, P. "Comparison between Thin Plate and Thick Plate from Navier Solution Using Matlab Software," *International Research Journal of Engineering and Technology (IRJET)*, 5(6), 2018, pp 2675 – 2680.

[7] Anon. "*Bending of Plates of Various Shape*," Thin Plates and Shells (2001). DOI:10.1201/9780203908723.ch5

[8] Onyeka, F.C. Okafor, F. O. and Onah, H. N. "Application of exact solution approach in the analysis of thick rectangular plate." *International Journal of Applied Engineering Research*, 14(8), 2019, pp 2043-2057.

[9] Onyeka, F. C. Okeke, E. T. Wasiu, J. "Strain–Displacement Expressions and their Effect on the Deflection and Strength of Plate," Advances in Science, *Technology and Engineering Systems*, 5(5), 2020a, pp 401-413. DOI: 10.25046/aj050551

[10] Kirchhoff, G. R. "Über Das Gleichgewicht Und Die Bewegung Einer Elastischen Scheibe," *Journal für die reine und angewandte Mathematik (Crelles Journal)*, 40, 1850, pp 51–88 (in German). DOI: 10.1515/crll.1850.40.51

[11] Ibearugbulem, O. M. "Use of Polynomial Shape Function in Shear Deformation Theory for Thick Plate Analysis," *IOSR Journal of Engineering*, 6(6), 2016, pp 8–20. DOI: 10.9790/3021-066010820

[12] Reissner, E. "The Effect of Transverse Shear Deformations on the Bending of Elastic Plates,

ASME," *Journal of Applied Mechanics* 12(2), 1945, pp A69-A77. DOI: 10.1115/1.4009435

[13] Mindlin, R. D. "Influence of Rotary Inertia and Shear on Flexural Motion of Isotropic Elastic Plates, ASME." *Journal of Applied Mechanics*, 18, 1951, pp 31 – 38. DOI: 10.1115/1.4010217

[14] Mantari, J.L., A.S. Oktem, and C. Guedes Soares. "A New Trigonometric Shear Deformation Theory for Isotropic, Laminated Composite and Sandwich Plates," *International Journal of Solids and Structures,* 49(1), 2012, pp 43–53. DOI:10.1016/j.ijsolstr.2011.09.008

[15] Sayyad, I. I. Chikalthankar, S. B. and Nandedkar, V. M. "Bending and free vibration analysis of isotropic plate using refined plate theory." *Bonfring International Journal of Industrial Engineering and Management Science*, 3(2), 2013, pp 40 – 46.

[16] Matikainen, M. K and Schwab, A. L. and Mikkola, A. M. "Comparison of two moderately thick plate elements based on the absolute nodal coordinate formulation. Multibody Dynamics," *ECCOMAS Thematic Conference K. Arczewski, J. Fra˛czek, M. Wojtyra (Eds.) Warsaw*, Poland, 29 June–2 July 2009.

[17] Hashemi, S.H., S. Farhadi, and S. Carra. "Free Vibration Analysis of Rotating Thick Plates" *Journal of Sound and Vibration*, 323(1-2), 2009, pp 366–384. DOI:10.1016/j.jsv.2008.12.007

[18] Pagano, N.J. "Exact Solutions for Rectangular Bidirectional Composites and Sandwich Plates," *Journal of Composite Materials* 4(1), 1970, pp 20-34, DOI: 10.1177/002199837000400102

[19] Uymaz, B. and Aydogdu, M. "Three-Dimensional Shear Buckling of FG Plates with Various Boundary Conditions." *Composite Structures*, 96, 2013, pp 670–682. doi: 10.1016/j.compstruct.2012.08.031

[20] Ibearugbulem, O.M., Onwuegbuchulem, U.C. and Ibearugbulem, C.N. "Analytical Three-Dimensional Bending Analyses of Simply Supported Thick Rectangular Plate," *International Journal of Engineering Advanced Research (IJEAR),* 3(1), 2021, pp 27-45.

[21] Onyeka, F. C. and Edozie, O. T. "Analytical Solution of Thick Rectangular Plate with Clamped and Free Support Boundary Condition Using Polynomial Shear Deformation Theory," *Advances in Science, Technology and Engineering Systems Journal*, 6(1), 2021a, pp 1427–1439. DOI: 10.25046/aj0601162

[22] Onyeka, F.C. Okafor, F. O. and Onah, H. N. "Buckling Solution of a Three-Dimensional Clamped Rectangular Thick Plate Using Direct Variational Method," *IOSR Journal of Mechanical and Civil Engineering (IOSR-JMCE)*, 18(3 Ser. III), 2021b, pp 10-22. DOI: 10.9790/1684-1803031022

[23] Onyeka, F.C., Osegbowa, D. and Arinze, E.E. "Application of a New Refined Shear Deformation Theory for the Analysis of Thick Rectangular Plates." *Nigerian Research Journal of Engineering and Environmental Sciences*, 5(2), 2020b, pp 901-917.

[24] Gwarah, L. S. "Application of shear deformation theory in the analysis of thick rectangular plates using polynomial displacement functions," *A published PhD.* Thesis Presented to the School of Civil Engineering, Federal University of Technology, Owerri, Nigeria, (2019).